Title	Magnetically mediated thermoacoustic imaging
Author(s)	Feng, Xiaohua; Gao, Fei; Zheng, Yuanjin
Citation	Feng, X., Gao, F., & Zheng, Y. (2014). Magnetically mediated thermoacoustic imaging. SPIE Proceedings, 8943, 894343-.
Date	2014
URL	http://hdl.handle.net/10220/20035
Rights	© 2014 SPIE. This paper was published in SPIE Proceedings and is made available as an electronic reprint (preprint) with permission of SPIE. The paper can be found at the following official DOI: http://dx.doi.org/10.1117/12.2041870. One print or electronic copy may be made for personal use only. Systematic or multiple reproduction, distribution to multiple locations via electronic or other means, duplication of any material in this paper for a fee or for commercial purposes, or modification of the content of the paper is prohibited and is subject to penalties under law.

Magnetically mediated thermoacoustic imaging

Xiaohua Feng*[a], Fei Gao[a], Yuanjin Zheng[a]

[a]School of Electrical and Electronics Engineering, Nanyang Technological University, Singapore 639798;

ABSTRACT

In this paper, alternating magnetic field is explored for inducing thermoacoustic effect on dielectric objects. Termed as magnetically mediated thermo-acoustic (MMTA) effect that provides a contrast in conductivity, this approach employs magnetic resonance for delivering energy to a desired location by applying a large transient current at radio frequency below 50MHz to a compact magnetically resonant coil. The alternating magnetic field induces large electric field inside conductive objects, which then undergoes joule heating and emanates acoustic signal thermo-elastically. The magnetic mediation approach with low radio frequency can potentially provide deeper penetration than microwave radiation due to the non-magnetic nature of human body and therefore extend thermoacoustic imaging to deep laid organs. Both incoherent time domain method that applies a pulsed radio frequency current and coherent frequency domain approach that employs a linear chirp signal to modulate the envelop of the current are discussed. Owing to the coherent processing nature, the latter approach is capable of achieving much better signal to noise ratio and therefore potential for portable imaging system. Phantom experiments are carried out to demonstrate the signal generation together with some preliminary imaging results. Ex-vivo tissue studies are also investigated.

Keywords: alternating magnetic field, thermoacoustic imaging, coherent frequency domain method, time domain method, magnetic coil

1. INTRODUCTION

Thermoacoustic imaging has undergone galvanizing progress in recent decades without sign of slowing down. Different spectrum of electromagnetic waves, including light[1-3], microwaves[4-6], have been used for inducing thermoacoustic effect for imaging and, due to the distinct interactions between these electromagnetic waves with matter, different contrasts for diagnosis are extracted. As a multi-wave imaging modality, it combines high contrast of dielectric property of the matter and good resolution of ultrasound. Specifically in microwave induced thermoacoustic imaging (MI-TAI), tissue absorbs a tiny amount of the incident pulsed microwave energy and subsequently emits ultrasonic waves thermal-elastically. Compared with photoacoustic imaging that uses light for excitation, it offers deeper penetration. Yet, the penetration is still not sufficient for deep laid lesions like early stage cancer in large breast. This is also true for high water (major microwave absorber) content tissues like skin and muscles. Depending on the microwave frequency being utilized, the estimated penetration depths[5] for muscles are 3.2 cm and 1.2 cm respectively at commonly used frequencies of 434MHz and 3GHz. Various exogenous contrast agents with enhanced microwave absorption are potential solutions for larger penetration[7-8]. However, lots of obstacles need be addressed before they can be translated into clinical usage, with one of the most prominent issues being the fact that their toxicity for humans remains only partially understood. In principle, far deeper penetration can be obtained by scaling down the frequencies to several tens MHz like 20 MHz, which offers at least 15 cm penetration. Unfortunately, antennas for efficient electromagnetic radiation at such frequency is comparable in size to human body and therefore it will be difficult to scale the irradiation region. Additionally, the conventional radiation approach tends to be inefficient in depositing electric field inside materials pertaining large permittivity, as discussed later.

To achieve a larger penetration depth and explore potentially a more energy efficient solution, we propose here to adopt magnetic field operating at radio frequency below 50 MHz for mediating thermoacoustic imaging. With a pulsed radio frequency magnetic field penetrating an dielectric matter, an alternating electric field is generated inside.

*xfeng1@e.ntu.edu.sg; phone +65 81695041;

Photons Plus Ultrasound: Imaging and Sensing 2014, edited by Alexander A. Oraevsky, Lihong V. Wang,
Proc. of SPIE Vol. 8943, 894343 · © 2014 SPIE · CCC code: 1605-7422/14/$18 · doi: 10.1117/12.2041870

Subsequent joule heating of the matter due to its finite conductively leads to transient thermal expansion of it, which ultimately gives rise to thermoacoustic signal emissions. The alternating magnetic field is appealing for mediating thermoacoustic effect because most objects, including human body, are non-magnetic and respond to magnetic field nearly as free space[9]. This implies a magnetically homogenous environment for the delivering field and it thus will circumvent the reflections existed in other incumbent radiation approaches, where more than 70% of total incident energy can be reflected before reaching the target. At the same time, using the non-radiant coil as the energy emitters is essentially an near field approach in which the magnetic field is immune from the large permittivity of the matter for depositing electric field therein, providing a more efficient solution in terms of energy conversion. Though the non-magnetic nature of human body implicates that the major source in the magnetically mediated thermoacoustic imaging of tissues will be electrical, magnetic sources can arise when foreign objects like steel and magnetic nanoparticles are present. Still, as these objects are embedded in a non-magnetic surroundings, the penetration depth is generally not affected. It is then meaningful to generalize the thermoacoustic sources to encompass both electrical and magnetic ones. Utilizing alternating magnetic field to heat magnetic nanoparticles for thermoacoustic imaging is recently considered theoretically in [10]. The theory presented here, however, is intended to be more general so that other magnetic materials like steel can be included.

2. THEORY

When a dielectric object is subjected to an alternating magnetic field, which can be generated by a compact magnetically resonance solenoid coil networked with additional capacitors, it will interact with both the magnetic field and the accompanying electric field, depending on its dielectric properties. Assume the radio frequency current flowing in the coil is $I(t)$ and the radius of the coil R is much smaller than the wavelength λ of the current so that the radiation is negligible, the magnetic field at location r and time t can be computed analytically with the law of Biot and Savart:

$$B(r,t)=\frac{\mu_0 NI(t)}{4\pi}\int\frac{dl'\times(r-r')}{|r-r'|^3}, \tag{1}$$

where N is the coil's number of turns, μ_0 is the permeability of the surroundings of the object and r' denotes the position of current element dl' of the coil. The alternating electric field E is then solved according to the Maxwell's equation: $\nabla\times E=-\frac{\partial B}{\partial t}$, which yields:

$$E(r,t)=\frac{\mu_0\omega NI(t)}{4\pi}\int\frac{dl'}{|r-r'|}, \tag{2}$$

where ω is the current radian frequency. Let the object conductivity be $\sigma(r)$ and its relative magnetic susceptibility be $\mu(r)=\mu'(r)+j\mu''(r)$, in which $\mu'(r)$ and $\mu''(r)$ denotes the real part and the imaginary part respectively. Then the object interacts with the electric field and produces a conductive current $J(r,t)=\sigma(r)E(r,t)$ inside, causing absorption of incident radio frequency energy through joule heating $H_J(r,t)=\langle J(r,t)E(r,t)\rangle=\langle\sigma|E|^2\rangle$. In the equation, operator $\langle\ \rangle$ denotes short time average and $|\ |$ represents absolute value. At the same time, the interaction of the object with the magnetic field gives rise to magnetic losses $H_M(r,t)=\langle\omega\mu''|B|^2/2\mu_0\rangle$. The magnetic losses encompasses that of magnetic nanoparticles by noting that the imaginary part of the relative magnetic permeability $\mu''(r)$ equals to the imaginary part of the magnetic susceptibility, that is, $\mu''(r)=\chi''(r)$. It is then observed that the magnetic losses calculated here is the same with that in [11]. The total heat function (absorbed energy per unit time and per unit volume) is the sum of the two components $H(r,t)=H_J(r,t)+H_M(r,t)$ and the consequent thermoacoustic wave equation is hence[12]:

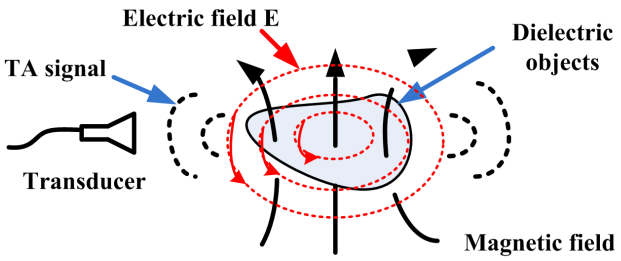

Figure 1. Schematic of magnetically mediated thermoacoustic generation

$$\nabla^2 p(r,t) - \frac{1}{c^2}\frac{\partial^2}{\partial t^2} p(r,t) = -\frac{\beta}{C_p}\frac{d}{dt} H(r,t), \tag{3}$$

where $p(r,t)$, c , β , C_p is respectively the thermoacoustic (TA) pressure, speed of sound, isobaric volume expansion coefficient and specific heat capacity of the object. The frequency domain method for thermoacoustic imaging is better illustrated with Fourier transforms. Taking the Fourier transform of the wave equation, it yields:

$$\nabla^2 P(r,\omega) + k^2 P(r,\omega) = -\frac{j\omega\beta}{C_p} H(r,\omega), \tag{4}$$

The corresponding solutions is then:

$$P(r,\omega) = -\frac{j\omega\beta}{4\pi C_p}\int \frac{e^{jk|r-r'|}}{|r-r'|} H(r,\omega) d^3 r', \tag{5}$$

where k is the acoustic wave number. The frequency domain method is essentially a match filter based coherent detection, a method widely used in radar and sonar applications. Specifically in magnetic mediated thermoacoustic imaging, it relies on the capability to modulate the heating function as implied in Eq.5: the resultant acoustic signals follows the heating function with certain weighting constant. The heating function, which is determined by the envelop of the electric and magnetic field (due to time averaging operation), can in turn be controlled by modulating the current magnitude flowing in the coil. With the current amplitude be modulated with chirp signals[13] or other codes[14], the TA signal will then be "coded" that allows subsequent correlation with the known modulation reference to achieve significant improvement in the signal to noise ratio (SNR). For example, consider the case that a chirp signal sweeping from ω_0 to ω_1 within a time duration T is used to modulate the amplitude of the radio frequency current. Assuming the amplitude of the reference is A_0 and received signal amplitude is A_1 and it is delayed by $\tau = \frac{|r-r'|}{c}$, then their cross-correlation is:

$$S(t) = \frac{A_0 A_1 T^2}{2\pi m(t-\tau)} \sin\left[\frac{m\pi(t-\tau)}{T}(1-\frac{t-\tau}{T})\right] \cos(\omega_c(t-\tau)), \tag{6}$$

where $\omega_c = {(\omega_0+\omega_1)}/{2}$ is the chirp center frequency and $m = (\omega_1 - \omega_0)T$ is the time-bandwidth product. The SNR improvement can be obtained is then $\sqrt{m}$, which can be scaled for catering to different applications. For instance, a burst chirp signal ranging from 0.5 MHz to 1.5 MHz that lasts 1 ms can yield an improvement in SNR by 31 times (30 dB). With a duty cycle of 10% for the burst chirp signal, the repetition rate can be 100 Hz, high enough for real time imaging (50~60 Hz).

As the heating function is proportional to the square of the electric field and magnetic field, it is crucial to have a efficient way for their deposition. For the far field radiation approach, a power density of Pd deposited into a medium with a permittivity of ε will produce an electric field: $E = 2\sqrt{{\mu_0}/{\varepsilon}} \times \sqrt{Pd} \propto \frac{1}{\sqrt{\varepsilon}}$. Being inversely proportional to the permittivity square root, the electric field will be degraded inside tissue compared to that in air since the former has a much larger permittivity. In contrast, the magnetic mediation is a near field approach and since normal objects, including human body, is transparent to magnetic field, the permittivity will not affect the electric field deposition. This can also be seen from Eq. 2, where only the permeability is shown to effect the electric field generation. The near field approach can

achieve a superior energy deposition is previously exploited in Ref. where the non-radiation near field energy, along with the far field radiation one, is utilized for thermoacoustic imaging. It is shown that a larger fraction of the energy is stored in the near field around the energy emitters rather than the far field. This is also the case in magnetic mediation approach, where the energy is most efficiently delivered near the coil. With a Helmholtz coil, the field in between is rather homogenous and it thus indicates a efficient and confined energy delivery. The penetration depth then is determined by the size of the coil, which can be scaled to image both deep laid objects with larger coils and smaller coil for superficial objects. Another point worth mentioning is that the relative low frequency utilized in magnetic mediation approach will make the specific absorption rate (SAR) smaller than microwave induced thermoacoustic imaging, as both the joule heating and magnetic losses are proportional to the frequencies being employed. It thus indicates a worse SNR, representing hence a tradeoff between SNR and penetration, as in ultrasound imaging and other thermoacoustic/photoacoustic imaging methods. Higher frequencies like 50 MHz, which can still provide sufficient penetration, can be used to improve the SAR for obtaining better SNR. More importantly, the coherent frequency domain method is able to enhance the SNR further.

3. EXPERIMENTAL RESULTS AND DISCUSSION

Experimental setup illustrated in figure 2 is used to demonstrate the signal generation and preliminary imaging capability of the magnetic mediation approach. Based on a similar setup reported previously[15], in which a larger customized Helmholtz coil with deeper penetration and the frequency domain method for improving SNR were demonstrated, the time domain method with a much smaller coil is now used to show the scalability of this method. Here, the customized coil has a diameter of 1 cm and a number of turns of 20. An RFID ferrite core is used to enhance the magnetic field by inserting it inside to coil.

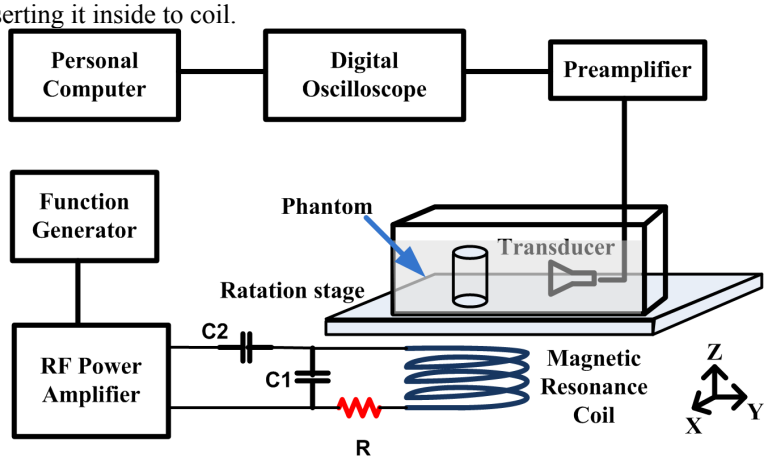

Figure 2. Experiment setup for magnetically mediated thermoacoustic signal generation and imaging

The radio frequency signal is produced by an arbitrary function generator (Tektronix, AFG3252) at repetition frequency of 1 kHz and then fed into the an RF pulse amplifier (BT00200-AlphaSA-CW, Tomcorf) for driving the resonance coil. The peak power can be generated by the power amplifier is 250 W. A 2.2 ohm resistor monitors the current flowing in the coil. The resonance frequency of the magnetic coil is 19.2 MHz and its associated quality factor is measured to be approximately 20. A focused ultrasound transducer (Olympus, V303) is used to detect the generated thermoacoustic signal, which is first amplified by a 54 dB low noise amplifier (model 5662, Olympus) and then digitized by the oscilloscope (Waverunner 6Zi, Lecroy). The data is averaged 1024 times, lowpass filtered with a cutoff frequency of 2 MHz by the oscilloscope, and then transferred to MATLAB 2010b on a PC for offline processing. The RF pulse width is set to 1 μs and the carrier frequency is 19.2 MHz, coinciding with the resonance frequency of the magnetic coil. At maximum output power, the peak current flowing in the coil is measured to be about 10 A. A round metal strip with diameter of 8 mm is used as the phantom to demonstrate thermoacoustic signal generation by the radio frequency pulses. It is erected and placed 0.3 mm above the coil. To form an image, the ultrasound transducer is fixed while the water tank and the phantom is mounted on a rotation stage. The signal is collected with 360 degrees coverage and a angle step of 5 degrees. The signal generated at the first angle without time gating is given in figure. 3 (a), where the distance between the transducer and phantom is around 3 cm. The signal appears at 20 μs, agreeing with the propagation delay. All the received signals are then time gated in Matlab to eliminate the direct electromagnetic interferences when do image reconstruction. The TA image shown in figure 4 is formed with a delay and sum algorithm[16], owing to its simplicity,

after envelop extraction of each A-line signal. The round anatomic structure is clearly distinguishable from the background. However, due to the finite bandwidth of the ultrasound transducer, the center part of the metal strip is not well rendered, as expected. It is also observed that the image is not a perfect circle. This is caused by slight transducer movements during rotation of the water tank in order to rotate the phantom.

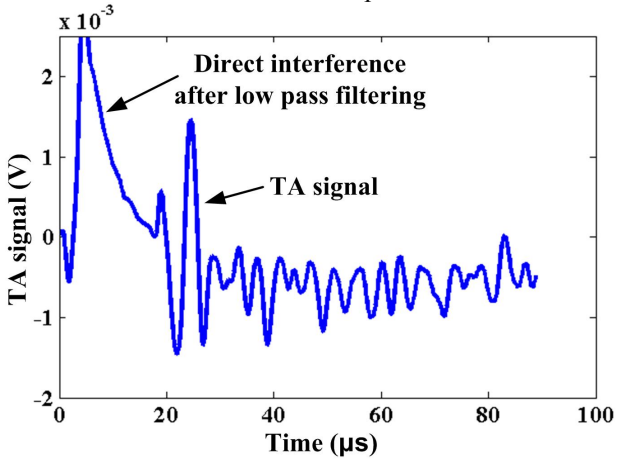

Figure 3. Detected TA signal at the first angle.

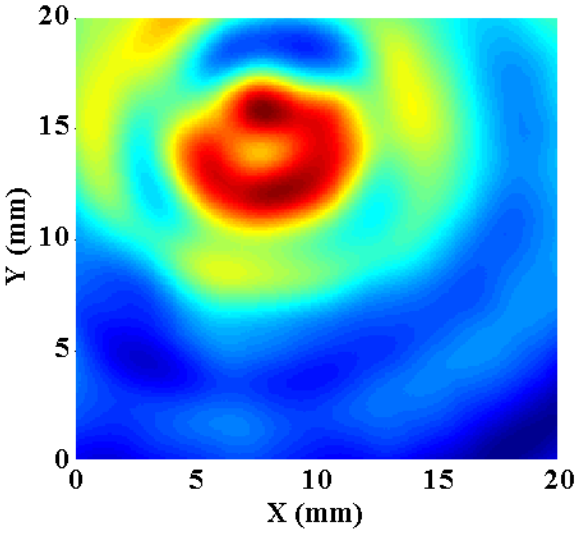

Figure 4. TA Tomography of a round metal strip.

When the metal strip phantom is replaced by a excised pork muscle, no thermoacoustic signal is observed. This is mainly due to the limited power that is used, which is 250 W, and the fact that the muscle absorbs the energy much less than the metal strip. Compared to microwave induced thermoacoustic imaging that generally employs several tens kilowatts[17-18], 250 W is a very low value. To tackle it, coherent frequency domain method can be used. The problem then is the direct electromagnetic interference that can override or mask the weaker thermoacoustic signal. In previous report, the chirp duration is made short enough to be smaller than the propagation delay between the imaged object and the receiving transducer so that this problem is circumvented. This solution can also be applied here but more generally, it requires good electromagnetic shielding. Another solution is to design a high order low pass filter before the low noise amplifier to eliminate the high frequency interference because the generated thermoacoustic signal is at the lower end. Another point worth mentioning is the quality factor of the resonance coil. A higher quality factor (Q) is desired to benefit from its current amplifying capability, however, it also necessitates a longer pulse to build up. This is again a tradeoff between power and resolution: higher Q gives more power for thermoacoustic signal generation but demands longer pulse to be used, which sacrifices resolution.

In summary, small end magnetically mediated thermoacoustic imaging is experimentally demonstrated with a frequency at 19.2 MHz. The round metal strip is imaged by delay and sum tomography algorithm with a high contrast.

The frequency in the magnetically meditated method can be scaled quite flexibly to be adapted into industrial and medical band (below 50 MHz) and the coil can be made to cater to different applications from imaging with large penetrations of several centimeters to imaging superficial objects with small area. For in-vivo imaging, much larger power is needed or the coherent frequency method should be adopted with a large time-bandwidth product. The imaging resolution can be scaled up relatively easily in the frequency domain method by adopting a higher center frequency for the chirp signal.

4. ACKNOWLEDGEMENTS

This research is supported by the Singapore National Research Foundation under its Exploratory/Developmental Grant (NMRC/EDG/1062/2012) and administered by the Singapore Ministry of Health's National Medical Research Council.

REFERENCES

[1] L. H. V. Wang, and S. Hu, "Photoacoustic Tomography: In Vivo Imaging from Organelles to Organs," *Science,* 335(6075), 1458-1462 (2012).
[2] D. Razansky, M. Distel, C. Vinegoni, R. Ma, N. Perrimon, R. W. Koster, and V. Ntziachristos, "Multispectral opto-acoustic tomography of deep-seated fluorescent proteins in vivo," Nat. Photon. 3, 412-417 (2009).
[3] Z. Yuan, and H. B. Jiang, "Quantitative photoacoustic tomography: Recovery of optical absorption coefficient maps of heterogeneous media," Appl. Phys. Lett. **88,** 231101(2006).
[4] C. G. Lou, S. H. Yang, Z. Ji, Q. Chen, and D. Xing, "Ultrashort Microwave-Induced Thermoacoustic Imaging: A Breakthrough in Excitation Efficiency and Spatial Resolution," Phys Rev Lett **109**, 218101 (2012).
[5] G. Ku, and L. H. V. Wang, "Scanning thermoacoustic tomography in biological tissue," Med. Phys. **27**, 1195 (2000).
[6] F. Gao, Y. J. Zheng, and D. F. Wang, "Microwave-acoustic phasoscopy for tissue characterization," Appl. Phys. Lett. **101**, 043702 (2012)
[7] M. Pramanik, M. Swierczewska, D. Green, B. Sitharaman, and L. V. Wang, "Single-walled carbon nanotubes as a multimodal-thermoacoustic and photoacoustic-contrast agent," J. Biomed. Opt. **14**(3), 034018 (2009).
[8] D. K. Kim, M. S. Amin, S. Elborai, S. H. Lee, Y. Koseoglu, M. Muhammed, and M. Muhammed, "Energy absorption of superparamagnetic iron oxide nanoparticles by microwave irradiation," J. Appl. Phys. **97,** 10J510 (2005).
[9] A. Karalis, J. D. Joannopoulos, and M. Soljacic, "Efficient wireless non-radiative mid-range energy transfer," Ann. Phys., New York, **323**, 34 (2008).
[10] D. Q. Piao, R. A. Towner, N. Smith, and W. R. Chen, "Magnetothermoacoustics from magnetic nanoparticles by short bursting or frequency chirped alternating magnetic field: A theoretical feasibility analysis," Med. Phys. **40,** 063301 (2013).
[11] R. E. Rosensweig, "Heating magnetic fluid with alternating magnetic field," J. Magn. Magn. Mate. **252,** 370 (2002).
[12] M. H. Xu, and L. H. V. Wang, "Time-domain reconstruction for thermoacoustic tomography in a spherical geometry," IEEE Trans. Med. Imaging. **21**, 814 (2002).
[13] S. Telenkov, A. Mandelis, B. Lashkari, and M. Forcht, "Frequency-domain photothermoacoustics: Alternative imaging modality of biological tissues," J. Appl. Phys. **105,** 102029 (2009).
[14] M. P. Mienkina, A. Eder, C. S. Friedrich, N. C. Gerhardt, M. R. Hofmann, and G. Schmitz, "Evaluation of Simplex Codes for Photoacoustic Coded Excitation," *4th European Conference of the International Federation for Medical and Biological Engineering*, 444 (2008).
[15] X. H. Feng, F. Gao, and Y. J. Zheng, "Magnetically mediated thermoacoustic imaging toward deeper penetration," Appl. Phys. Lett., 108, 083704 (2013).
[16] C. G. A. Hoelen, and F. F. M. de Mul, "Image reconstruction for photoacoustic scanning of tissue structures," Appl. Opt. 39, 5872-5883(2000).
[17] D. R. Bauer, X. Wang, J. Vollin, H. Xin, and R. S. Witte, "Spectroscopic thermoacoustic imaging of water and fat composition," Appl. Phys. Lett. **101**, 033705 (2012).
[18] A. Mashal, J. H. Booske, and S. C. Hagness, "Toward contrast-enhanced microwave-induced thermoacoustic imaging of breast cancer: an experimental study of the effects of microbubbles on simple thermoacoustic targets," Phys. Med. Biol. **54**, 641 (2009).